*PRAJÑĀ* - Journal of Pure and Applied Sciences Vol. 26 : 86 – 95 (2018)
ISSN 0975 - 2595

# CLEANING STRATEGIES FOR FLUX RECOVERY OF NANOFILTRATION MEMBRANE FOR ETHYLENE GLYCOL-SALT--WATER TERNARY MIXTURE

TEJAL M PATEL*, HARESH K DAVE AND KAUSHIK NATH
Department of Chemical Engineering, G H Patel College of Engineering & Technology
Vallabh Vidyanagar-388120, Gujarat, India
Email: tejalpatel@gcet.ac.in

**Abstract**

***The success of a membrane filtration process largely depends on employing an effective and efficient membrane cleaning method. Different cleaning strategies are explored in the present work to recover the permeate flux of a flat sheet nanofiltration membrane employed in the separation of ethythelne glycol from industrial wastewater. Chemical cleaning was carried out with 2% each of citric acid, EDTA and STPP solutions. The effectiveness of these chemicals as a cleaning agent was studied and flux recovery was calculated. The flux recovery after cleaning with citric acid, EDTA and STPP solutions were found out to be 69.84, 55.77., and 47.85% respectively. The surface morphology and functionality of the pristine and used membrane samples were also characterized by SEM, FTIR and AFM analysis.***

***Keywords: membrane fouling, flux decline, concentration polarization, chemical cleaning***

## 1. Introduction

Endowed with a number of advantages to its credit, membrane technology has become one of the most important industrial separation techniques to be applied extensively to various fields including the recovery of valuable products from wastewater. Among various pressure driven membrane processes nanofiltration in particular, has led to significant innovation in the recent past for the treatment of large amount of aqueous stream, which contain many different components with low molecular weight ranging from hundreds to thousands of Daltons such as inorganic/organic salts, amino acids and peptides, oligosaccharides, molasses, reactive dyes and so on [1,2,3]. Although the membranes can be operated at their optimal operating conditions, the fouling at a membrane surface seems to be an unavoidable phenomenon. Thus the success of a membrane filtration process largely depends on employing an effective and efficient membrane cleaning method. Membrane cleaning is of critical importance for the efficient recovery of the membrane's flux (throughput) and selectivity – the two most important performance indices of membrane separation [4, 5]. Cleaning also ensures the reuse of membrane for long term cost effective operation. The limited thermal and chemical robustness of membranes constrain cleaning methods to avoid frequent membrane replacement. There are quite a few numbers of physical and chemical cleaning methods depending upon the nature of the feed or foulants [6].

Physical cleaning of porous membranes includes hydraulic cleaning which consists of flushing (forward) and backwashing or backpulsing. This is one of the easiest cleaning methods, and nowadays is widely used in membrane bio reactors (MBR) and other cross flow operations [7, 8]. Regular intermittent backwash leads to the lift-off of deposited particles from the membrane surface and minimizes the extent of concentration polarization. Forward flushing can be undertaken during the filtration cycle with a backwash to improve shear and remove particle concentration build-ups. Backpulsing (also called backshocking) is a more rapid backwash with a forward filtration step and followed by a reversed filtration step. The pneumatic cleaning of the membrane consists of air sparging, air lifting, air scouring, and air bubbling [9, 10]. Air or inert gas is applied for direct cleaning or to enhance flux in the filtration step. This process has the advantage of low maintenance cost, ease of integration with the existing system, and elimination of cleaning chemicals. However, the disadvantages of air sparging include limited effectiveness in cleaning and the high pumping cost [11, 12]. The combined cleaning of air sparging and hydraulic backflush is also applied in many processes. Low frequency ultrasound irradiation (up to 40 kHz) is an effective cleaning strategy for fouled membranes. Ultrasonic waves create cavitation

and induce acoustic streaming, which provide vigorous mixing to breaking concentration polarization and cake layer on the membrane surface [13, 14].

When selecting cleaning conditions, one of the most important considerations is if the conditions for cleaning are compatible with membrane media and other components of the membrane filters and systems. Chemical compatibility of membrane and other filter components and systems limits the type and the maximum allowable concentration of a chemical to be used during cleaning [7]. Membranes made from materials with high chemical resistance allow more flexible selections of the type and the concentrations of cleaning chemicals in dealing with various types of fouling problems. Concentration of cleaning chemicals can affect both the equilibrium and the rate of reaction. Unlike reactions occurred in liquid phase, reactions between cleaning chemicals and fouling materials occur in the interface of liquid and a (solid) fouling layer. The concentration profile of cleaning chemicals within the fouling layer is a function of the concentration of cleaning chemicals in the bulk liquid phase. Therefore, the concentration of cleaning chemicals not only needs to maintain the reasonable reaction rate, but also needs to overcome mass transfer barrier imposed by the fouling layer [15]. In general, 5-20% of the operating costs of a large plant are associated to membrane cleaning procedures (Madaeni et al., 2001) [16]. Therefore, an intense research work is being done to develop new cleaning methods

A current practice of membrane cleaning is based on recommendations from membrane manufacturers which may consume more cleaning chemicals since the recommendations are given based on feed water quality, and are not based on severity of fouling. In addition, these chemicals are also quite costly [7, 17]. Membrane cleaning processes are not well automated and there is an opportunity to develop an advanced tool for estimating effectiveness of the membrane cleaning and optimizing of the cleaning operation. Therefore, a simple alternative method to identify the effectiveness of the membrane cleaning would be helpful. By estimating the effectiveness of the membrane cleaning, the cleaning chemical consumption and the plant down time can be minimized. Keeping this in mind different cleaning strategies were explored in the present work for a flat sheet nanofiltration membrane after using in the separation of ethylene glycol from wastewater. Chemical cleaning was carried out using citric acid, EDTA and sodoium tripolyphosphate. Physical cleaning methods involved were back and forward flushing with water and low frequency ultrasonic irradiation. Flux recovery was evaluated after each cleaning cycle to assess the reusability of the membrane. The pristine and fouled membranes were also analyzed using scanning electron microscopy, Fourier-transform infrared spectroscopy, and atomic force microscopy.

## 2. Materials and methods

### *2.1 Chemicals and reagents*

Citric acid (pH: 2.5), ethylene diamine tetra-acetic acid (EDTA) (pH: 8), and sodium tripolyphosphate (STPP) (pH: 9.8) were the cleaning reagents for the present study. Ethylene glycol (EG) containing wastewater was procured from M/s PCP Chemicals Pvt Limited, Mumbai, India. The important composition of wastewater is presented in Table 1. All the chemicals used in this study were of AR grade, supplied by Merck, India and were used as received without further purification. Deionized water (resistivity18 $M\Omega \cdot cm^{-1}$ at 25°C) was used for preparing stock solution.

### *2.2 Membrane*

Hydrophilized polyamide (PA-NF) membrane having molecular weight cut-off of 150 was used in the present study. The membrane was supplied by M/s Permionics Membrane Pvt. Ltd, Baroda, India. PA-NF membrane has three layers, which are fabric backed polysulfone UF support, interfacially coated with polyamide layer and then hydrophilized using Permionics proprietary additives. The average pore sizes and effective area of the membrane were 6±1 nm and 0.016 $m^2$ respectively. The key physico-chemical and performance properties of the PA-NF

membrane are listed in Table 2. The water permeability of the membrane was estimated to be $2.99 \times 10^{-11}$ $m^3/m^2sPa$.

*2.3 Experimental set-up and operating conditions*

The details of experimental setup and the schematic diagram are available elsewhere[18].Wastewater sample, diluted 5 times using deionised water, was passed through the membrane module at 490 kPa trans-membrane pressure for 90 minutes. The volume of feed solution was 25 l in the feed tank. Permeate samples were collected at fixed time intervals and concentration of the same were measured using Karl Fisher Apparatus. TDS and Conductivity of the samples were also measured using TDS meter (Hanna Instruments, Taiwan). All the experiments were conducted at the prevailing ambient temperature of 32±2°C.

*2.4 Chemical Cleaning*

Membrane cleaning was performed by immersing used membrane in the cleaning solution at ambient temperature kept overnight. The cleaning solution involved 2% by vol of citric acid, EDTA and sodium tripolyphosphate. The membrane swatches from the cleaning solution were subsequently rinsed with deionised water before placing it into the module.

*2.5 Physical Cleaning*

Physical cleaning of the membranes were accomplished in situ using forward and backward flushing with water for 1 h at ambient temperature. In forward flushing, water was passed in the same direction of feed flow while in back flushing, the flow direction was reversed. Cleaning of fouled membranes was also carried out ex situ by employing low frequency (25 kHz) ultrasonic irradiation for different intervals. After each cycle of cleaning, flux recovery ($F_r$) of the cleaned membrane was estimated using Eq.(1)

$$F_r = \frac{J_{w1}}{J_w} \times 100 \qquad (1)$$

Where, $F_r$ = flux recovery, $J_{w1}$ = Pure water flux after cleaning, $J_w$ = Pure water flux of unused membrane

*2.6 Determination of permeate flux and membrane rejection coefficient*

Permeate flux ($J_w$) of the membrane was determined using following relation

$$J_w = \frac{Q_p}{A} \qquad (2)$$

where $Q_p$ is the permeate flow per h and 'A' is the active surface area of the membrane ($m^2$). Membrane rejection coefficient (R) was estimated by

$$R = (1 - \frac{C_p}{C_b}) \times 100 \qquad (3)$$

Where $C_p$ is the concentration of the permeate and $C_b$ is the bulk concentration.

*2.7 Scanning electron microscopy*

The scanning electron microscopy (SEM) analysis of the pristine (unused) and fouled membranes was done on Leo 1430VP (England). All membrane samples were dried overnight at 40 °C before preparing 3 mm × 3 mm strips for silver sputter coating. The silver-coated strips were used for recording the SEM images.

*2.8 Fourier transform infrared spectros*copy (FTIR)

The surface organic functional groups of the membranes were studied by the Fourier transform infrared spectroscopy (Perkin Elmer Spectrum GX). The spectra were recorded from a wave number of 400 – 4000 $cm^{-1}$ at a resolution of 4.0 $cm^{-1}$ with an acquisition time of 1 min. Infrared absorption spectra are usually obtained by placing the sample in one beam of a double-beam infrared spectrophotometer and measuring the relative intensity of transmitted (and therefore absorbed) light energy versus wavelength (or wave number). A common light source for infrared radiation is the Nernst glower, a molded rod containing a mixture of zirconium oxide, yttrium oxide and erbium oxide that was

heated to around 1500ºC by electrical means. Wet samples were prepared by thoroughly cleaning virgin membrane coupons with deionized water and soaking them in a water bath for 24 h. Samples were then dried in a vacuum drier before analysis. The membrane active layers were pressed tightly against the crystal plate, and carbon dioxide and water vapor were removed during the measurements. At least 2 replicates were obtained for every sample type without applying any baseline corrections.

*2.9 Atomic force microscopy*

Atomic force microscopy (AFM) was carried out using a NT-MDT NTEGRA Aura Autoprobe CP atomic force microscope. Measurements were performed on dry membrane samples under ambient atmospheric conditions. Silicon cantilevers with integrated pyramidal tips were used to image membrane surface topography. The membrane surfaces were imaged in a non-contact or tapping (intermittent contact) mode. Differences in the membrane surface morphology were expressed in terms of various roughness parameters such as average roughness and root means square (RMS) roughness calculated from the AFM images using an AFM software program. The surface roughness was reported in terms of the root mean square roughness (RMS) and calculated by using Eq. (4)

$$RMS = \sqrt{\frac{\sum (Z_{cu} - Z_{av})^2}{p}} \quad (4)$$

where $Z_{av}$ is the average of the z values within the given area; $Z_{cu}$ is the current z value; and p is the number of points within a given area. The surface roughness parameter was calculated from the AFM images using an AFM software program.

## 3. Results and discussion

*3.1. Chemical cleaning*

In chemical cleaning, the choice of the cleaning agent assumes paramount importance. The optimal selection of the cleaning agent depends mainly on membrane material and type of foulants. These agents must be able to dissolved most of the deposited materials on the surface and removed them from the surface without causing any structural damage. In general, acids are often used to remove precipitated salts or scalants, while alkaline cleaning is suitable for organic fouling removal [2, 4]. Since the feed solution in the present study consisted predominantly of ethylene glycol and sodium sulphate, we selected citric acid (CA), EDTA and sodium tripolyphosphate (STPP) to study their suitability in flux recovery. Volumetric flux of pure water and EG wastewater as a function of time is presented in Figure.1.

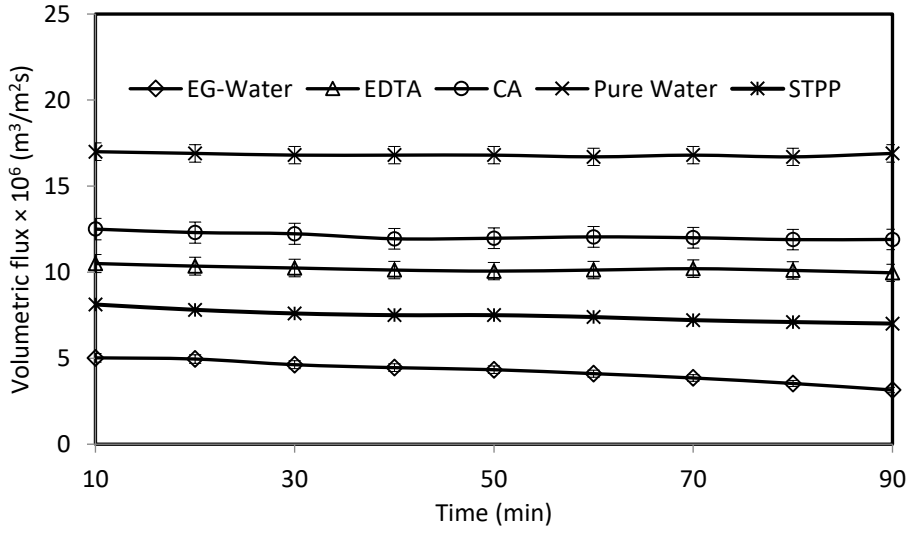


**Fig. 1.** Volumetric flux of permeate as a function of time for pure water, EG wastewater and pure water after chemical cleaning with different cleaning agents (trans-membarne pressure 490 kPa; Temp: 32±2ºC; Run Time: 90 min. cross flow velocity: 0.45 $ms^{-1}$)

In the same figure the recovered water flux of cleaned membranes with cleaning agents EDTA, CA and STPP are also compared. A perusal of Figure 1 indicates that for pristine membrane the pure water flux was almost steady throughout the runtime. But with diluted wastewater the flux was observed to decline after 30 min of operation. The initial flux was found out to be $5.02 \times 10^{-6}$ $m^3/m^2s$ which was reduced to $3.15 \times 10^{-6}$ $m^3/m^2s$ after 90 min of operation. This corresponds to about 62.7% reduction of flux.

Pure water flux recovery after cleaning with citric acid was 69.84%. When the fouled membrane was cleaned with citric acid, it might have dissolved the deposited salts on the membrane surface thereby removing the adsorbed salts from the membrane, This is because of the fact that cleaning is generally a combination of two factors—the dissolution or desorption effect of the cleaning agent, and the hydrodynamic shear stress applied to the foulant layer [19]. Since the salts adsorbed on the membrane surface blocking the pores, are removed, the solvent passage through the membrane was facilitated with subsequent increase in permeate flux.

Flux recovery after cleaning with EDTA and STPP were estimated to be 55.77% and 47.85% respectively. Figure 1 indicates that the flux recovery was more with citric acid as compared to EDTA and STPP. This may be due to the better ability of dissolving or more interactions of the solutes with citric acid solution. EDTA can also form some complexes with the solutes and hence the solutes could be detached from the membrane. However, in the present experiment the EDTA solution with pH 8.0 and STTPP with pH 9.8 were found to be not much effective in dissolution of the deposited salts. The water flux was not completely recovered as the initial flux, due to adsorption and permanent fouling.

### *3.2. Forward and backward flushing*

Physical cleaning of membrane was carried out by using forward and backward flushing of water across the membrane surface in the flat sheet module. In forward flushing water was pumped at high cross-flow velocity ($0.45$ $ms^{-1}$) through the feed side in order to remove foulants from the membrane surface. Because of the more rapid flow and the resulting turbulence, particles absorbed on to the membrane were released and discharged. In the reverse flushing method, permeate direction was reversed to flush the membrane backwards from permeate side to feed side. The deposited foulants were expelled by the inversed pressure and were then removed out of the membrane module by the reject stream. Reversible fouling caused by loosely adsorbed solute particles could be removed in this process. In forward flushing flux recovery was found out to be 80.97%, whereas in backward flushing it was 89.1%. Backward flushing was more effective for controlling flux decline than increasing shear stress on membrane; because shear stress reduced concentration polarization but back flushing could reduce both external and internal fouling [20]. In case of backward flushing from the permeate to the feed end of the membrane, it results in expansion of the thickness of the fouling layer. After this, a forward flush is usually used to wash out the detached layer or dilute the fouling layer. However to obtain the best performance optimization of the two flows (forward flow and backflow) are required. However, the frequency, duration and backwashing flux are the crucial parameters for fouling mitigation. Backwashing sometimes might affect the production efficiency of permeate stream. [5]. However, these are not studied in the present work.

### *3.3. Ultrasonic irradiation*

Application of ultrasound for mitigation of flux decline during nanofiltration of dye solution has been extensively studied by our research group [3]. Acoustic irradiation is widely considered as an effective pretreatment to minimize fouling specially due to particulate or organic matter. For ultrasonic membrane cleaning the used membranes were subjected to low frequency (25 kHz) ultrasonic irradiation for a period of 2, 4, 6, and 8 min. With increasing in the duration of exposure to irradiation the flux recovery was increased as shown in Figure 2. Flux recovery, after 2, 4, 6

and 8 min were calculated to be 54, 80 92 and 95% respectively. Irradiation was not continued beyond 8 min as there were chances of cracks on the membrane surface.The basic physical phenomenon behind the effect of ultrasound is cavitation, that starts between this range of frequency, and is promoted by the passage of the ultrasound waves through the liquid medium in a series of alternate compression and expansion cycles. Cavitation mainly promotes formation, growth and implosive collapse of bubbles in the liquid that has significant mechanical and chemical effects. In fact, it is reported that each cavitation bubble generates temperatures of 4000-6000 K and pressures of 100-200 MPa, acting as active "hot spots" (Feng et al., 2006) [21].The acoustic streaming and shear forces imposed by cavitation bubbles reduce the fouling on membrane surface.

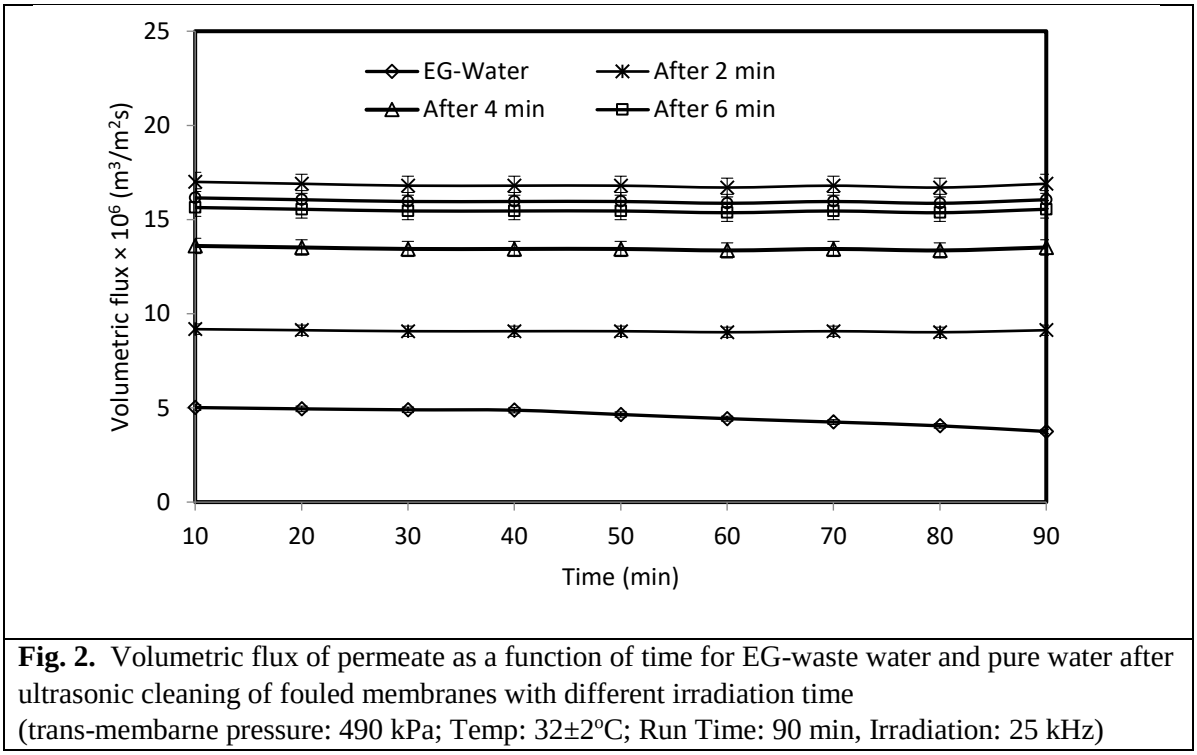


**Fig. 2.** Volumetric flux of permeate as a function of time for EG-waste water and pure water after ultrasonic cleaning of fouled membranes with different irradiation time
(trans-membarne pressure: 490 kPa; Temp: 32±2°C; Run Time: 90 min, Irradiation: 25 kHz)

*3.4. SEM analysis*

Figure 3 presents SEM micrographs of the pristine and used membrane samples from the experiments. The surface of the pristine membrane has a denser and tighter network of cellular pores and contained a network of ridges and valleys, which could conceivably trap organic molecules and inorganic salts, such as those believed to cause fouling on the membrane surface. It is obvious that the membrane had an asymmetrical structure consisting of a dense skin layer and a porous sub layer that was occupied by cellular morphologies enclosed in polymer matrix. The skin layer is responsible for the permeation or rejection of solutes, whereas the porous bulk acts only as a mechanical support. The top layer of the pristine membrane, as found from the microgram consisted of a closely packed layer of nodules.SEM images of used membranes were markedly different from those of new membranes. The micrograph of used membranes showed a cake of colloidal particles similar to fine sand or silt. This fouling layer completely occluded the active surface of the membrane. The SEM images also show that the foulant layer was having significant roughness and was textured. Generally speaking, the surface roughness of the different types of membrane is shown to differ based on the number of the peaks and valleys, peaks width and height. This morphological difference is likely caused by differences in the diffusion rate of amine monomers during the interfacial polymerization [22].

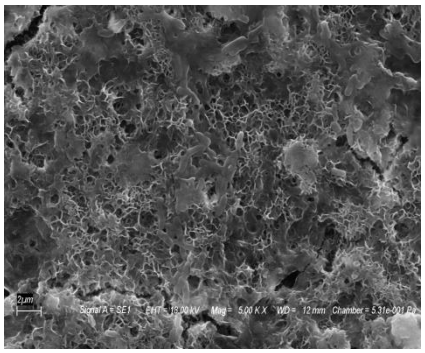

**Fig. 3.** SEM micrographs

*3.5 FTIR Analysis*

A closer insight of the surface functional groups was obtained by comparing FTIR spectra of pristine membrane with that of the used one as presented in Figure 4. The principal absorption bands for the virgin membrane consist of frequencies or wave numbers associated with these bond characteristics are N–H stretching vibration at 3438.49, 3440.87 $cm^{-1}$; C−H stretching in aliphatic structure ($-CH_2-CH_2-CH_3$) at 2925.62, 2926.31 $cm^{-1}$, N–H bending vibration due to amine at 1632.06, 1633.93 $cm^{-1}$, and C–C multiple bend stretching due to aromatic at 1410.29 and 1411.23 $cm^{-1}$ [23]. From the FTIR spectra for the fouled membrane it can be seen that the absorption peaks in the used membrane spectra were either eliminated or severely attenuated due to salt deposition. Moreover there were few additional absorption peaks detected at wave numbers of 725, 794, 871, 1664, and 1725 $cm^{-1}$ in the spectra of the fouled membrane. The spectral bands between wave numbers 950 and 1200 $cm^{-1}$ were significantly stronger in intensity for the membrane fouled with EG- water, as compared to the virgin membrane [24]. This peak apparently originated from the di-alcohol O–H bending vibration at 1245.97 $cm^{-1}$. However, more information about the chemical bonding signatures could not be obtained from the spectral analysis. These differences might be due to the different composition of the proprietary layer structure of the commercial membrane used in the present study. About the more detailed relationship between the materials of the pristine membrane used and fouled membrane need further study. It merits mentioning that a few absorptions detected near 3770 $cm^{-1}$ were probably due to water molecules as a result of inadequate drying of the test sample. These absorptions might have obscured some of the expected bands leading to erroneous assignments of a few bands.

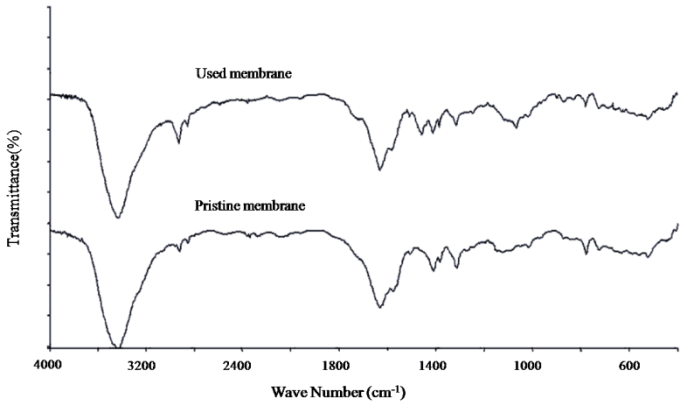


**Fig. 4.** FTIR Spectra of the pristine and used membrane from the present study

*3.6 AFM analysis*

The topology and texture of the

membrane sample surfaces were investigated using atomic force microscopy (AFM) technique. AFM involves measurement of surface atomic forces to image three-dimensional topographical maps of the surface with high resolution. Representative orthographic plots of tapping mode AFM images of pristine membrane, fouled membrane, and cleaned membranes by chemical and physical cleaning are presented in Figure.5. The surface roughness parameters of the membranes obtained from AFM images using SPM DME software are given in Table 3. The roughness parameters are expressed in terms of the mean roughness ($S_1$), and the root mean square (RMS) roughness of the Z data ($S_2$). A close inspection of AFM micrographs from Figure.5 indicates that the surfaces of all the membranes have a "ridge-and-valley" morphology. Occurrence of deep depressions on the membrane surface represents pores whereas the high peaks correspond to nodules. Both these conditions lead to high roughness parameters. However, for a rough membrane, particles are preferentially transported into the valleys. The valleys quickly become clogged with multiple layers of densely packed particles increasing the cumulative resistance to flow in the valleys and leading to a more rapid loss of flux than for a smooth membrane [25]. A perusal of Table 3 indicates that both mean and rms roughness of the fouled membrane were much higher than the pristine membranes. Even though after cleaning the values of roughness decreased, those were still higher than the original roughness values of the unused membranes. The increase in surface roughness was due to the accumulation of solute particles in the concavities of membrane surfaces. Solutes accumulated in such a densely compacted layer that even defouling by chemical or physical cleaning could fail to recover the original roughness values. The pores in the virgin membrane were completely masked by residual foulants and it was evidenced from the consistent flux deterioration during the course of experiments. Moreover there were not much morphological differences between the surface topography of the chemically cleaned membrane with that cleaned by physical method.

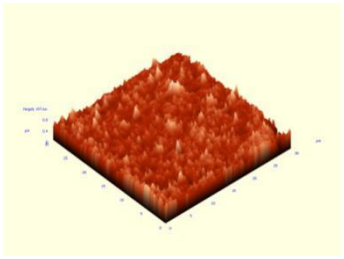

(a) Pristine membrane

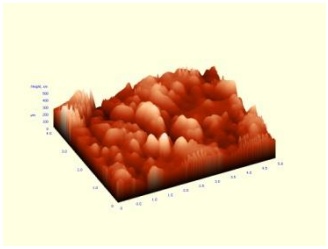

(b) Fouled membrane

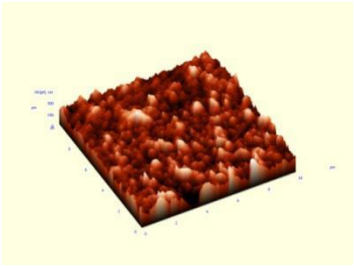

(c) Chemically cleaned membrane

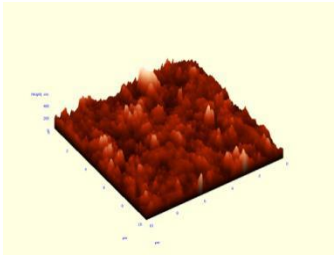

(d) Physically cleaned membrane

**Fig.5.** AFM micrograph of membranes used in the present study.

## 4. Conclusion

Membrane cleaning experiments indicate that in chemical cleaning with dilute citric acid (CA) the flux recovery was 69.84% which was higher than the percent recovery obtained with other two chemicals. CA was more effective than the EDTA and STPP solutions for recovering pure water permeability. In forward and backward flushing flux recoveries were found out to be 80.97% and 89.1% respectively. However the maximum flux recovery of 95% was achieved with ultrasonic cleaning for a time span of 8 min. The SEM micrograph of fouled membranes showed a layer of silt like colloidal particles which almost completely occluded the active surface of the membrane. Absorption peaks in the FTIR spectra of the used membrane were appeared to be either eliminated or severely attenuated due to salt deposition. Mass transfer barriers within the fouling layer are likely to be the rate-limiting factor, which are required to be analyzed in depth. Creating favorable hydrodynamic conditions to facilitate mass transfer is likely to enhance the efficiency of cleaning. The chemical cleaning agents tested could not achieve complete flux recovery because residual foulants were strongly embedded in the concavities of membrane surfaces, as reflected by AFM studies.

## Acknowledgement

The authors are grateful to Gujarat Council on Science and Technology (GUJCOST), Department of Science & Technology, Government of Gujarat, India for providing grant (File No: GUJCOST/MRP/2015-16/2714) to carry out the work and Sophisticated Instrumentation Centre for Applied Research & Testing (SICART), Vallabh Vidyanagar for carrying out certain analyses.

## References

[1] Al-Amoudi.A, and Lovitt. W.L (2007), "Fouling strategies and the cleaning system of NF membranes and factors affecting cleaning efficiency", J. Membr. Sci.,303, 4-28.

[2] Arnal.J.M, Garcia-Fayos.B, Sancho.M, and Verdu.G (2009), "Ultrafiltration membrane cleaning with different chemical solutions after treating surface water", *Desalination and Water Treatment*, **7**, 198-205.

[3] Patel.T.M, and Nath.K (2013), "Alleviation of flux decline in cross flow nanofiltration of two-component dye and salt mixture by low frequency ultrasonic irradiation", *Desalination*, 317, 132-141.

[4] Porcelli.N, and Judd.S (2010), "Chemical cleaning of potable water membranes: A review", *Sep Purif Technol*, 71, 137-143.

[5] Chen.J.P, Kim.S.L and Ting.Y.P (2003), "Optimization of membrane physical and chemical cleaning by a statistically designed approach", *J. Membr. Sci.,* 219 27–45.

**[6]** Liu.C, Caothien.S, Hayes.J, Caothuy.T, Otoyo.T and Ogawa.T (2001), "Membrane chemical cleaning: from art to science", *Proceedings of 2001 Membrane Technology Conference*, AWWA.

[7] Liikanen.R, Yli-Kuivila.J and Laukkanen.R (2002), "Efficiency of various chemical for nanofiltration membrane fouled by conventionally-treated surface water", *J. Membr.Sci.,* **195**, 265-276.

[8] Smith.P.J, Vigneswaran.S, Ngo.H.H, Ami,R.B and Nguyen.H (2006), "A new approach to backwash initiation in membrane systems", *J. Membr. Sci.,* **278**, 381–389.

[9] Psoch.C and Schiewer.S (2006), "Resistance analysis for enhanced wastewater membrane filtration", *J. Membr. Sci.,* **280**, 284–297.

[10] Cornelissen.E.R, Vrouwenvelder.J.S, Heijman.S.G.J, Viallefont.X.D, van Der Kooij.L and Wessels.L.P (2007), "Periodic air-water cleaning for control of biofouling in spiral wound membrane elements", *J. Membr. Sci.,* **287**, 94–101.

[11] Ducom.G and Cabassud.C (2003), "Possible effects of air sparging for nanofiltration of salted solutions", *Desalination*, **156**, 267-274.

[12] Cui.Z and Taha.T (2003), Enhancement of

ultrafiltration using gas sparging: a comparison of different membrane modules", *J. Chem Tech.Biotech,* **78**, 249-253.

[13] Muthukumaran.S, Yang.K, Seuren.A, Kentish.S, Ashokkumar.M, Stevens.G.W and Grieser.F (2004), "The use of ultrasonic cleaning for ultrafiltration membranes in the dairy industry", *Sep. Purif. Technol.* 39, 99–107.

[14] Juang.R.S and Lin.R.H (2004), "Flux recovery in the ultrafiltration of suspended solutions with ultrasound", *J. Membr. Sci.,* 243, 115-124.

[15] Lee.H.J, Amy.G, Cho.J, Yoon.Y, Moon.S.H and Kim.I.S (2001), "Cleaning strategies for flux recovery of an ultrafiltration membrane fouled by natural organic water", *Water Res*., **35**, 301–3308.

[16] Madaeni.S.S, Mohamamdi.T and Moghadam.M.K (2001), "Chemical cleaning of reverse osmosis membranes", *Desalination,* **134**, 77-82.

[17] Lin.J.C.T, Lee .D.J and Huang.C (2010), "Membrane fouling mitigation: Membrane cleaning" *Sep. Sci. Technol.,* **45**, 858-872.

[18] Patel T.M, Chheda.H, Baheti.A, Patel.P and Nath.K (2012), "Comparative performance of flat sheet and spiral wound modules in the nanofiltration of reactive dye solution", *Environ Sci Pollut Res*., **19**, 2994–3004.

[19] Song.W, Ravindran.V, Koel.B.E and Pirbazari.M (2004), "Nanofiltration of natural organic matter with $H_2O_2$/UV pretreatment: fouling mitigation and membrane surface characterization", *J. Membr. Sci.*, **241**, 143–160.

[20] Sagiv.A and Semiat.R (2010), "Parameters affecting backwash variables of RO membranes", *Desalination,* **261**, 347-353.

[21] Feng.D, Van Deventer. J.S.J and Aldrich.C (2006), "Ultrasonic defouling of reverse osmosis membranes used to treat wastewater effluents", *Sep. Purif. Technol.*, **50**, 318–323.

[22] Liu.Y, Zhang.S, Zhou.Z, Ren.J, Geng.Z, Luan.J and Wang.G (2012), "Novel sulfonated thin-film composite nanofiltration membranes with improved water flux for treatment of dye solutions", *J Membr. Sci.*, **394– 395**, 218– 229.

[23] Tang.C.Y, Kwon.Y.N and Leckie.J.O (2009), "Effect of membrane chemistry and coating layer on physiochemical properties of thin film composite polyamide RO and NF membranes .FTIR and XPS characterization of polyamide and coating layer chemistry", *Desalination*, **242**, 149–167.

[24] Dyer.J.R (2012), "Applications of Absorption Spectroscopy of Organic Compounds", *PHI Learning Pvt. Ltd., New Delhi,* 23–41.

**[25]** Hoek.E.M.V, Bhattacharjee.S and Elimelech.M (2003), "Effect of membrane surface roughness on colloid-membrane DLVO interactions", *Langmuir*, **19**, 4836–4847.